TOPICAL REVIEW — Topological electronic states

Two-dimensional topological insulators with large bulk energy gap*

Z Q Yang(杨中强)[1,2], Jin-Feng Jia(贾金锋)[1,2], and Dong Qian(钱冬)[1,2,†]

[1] *Key Laboratory of Artificial Structures and Quantum Control (Ministry of Education), Department of Physics and Astronomy, Shanghai Jiao Tong University, Shanghai* 200240, *China*

[2] *Collaborative Innovation Center of Advanced Microstructures, Nanjing* 210093, *China*

(Received 14 July 2016; revised manuscript received 9 September 2016; published online 28 September 2016)

Two-dimensional (2D) topological insulators (TIs, or quantum spin Hall insulators) are special insulators that possess bulk 2D electronic energy gap and time-reversal symmetry protected one-dimensional (1D) edge state. Carriers in the edge state have the property of spin-momentum locking, enabling dissipation-free conduction along the 1D edge. The existence of 2D TIs was confirmed by experiments in semiconductor quantum wells. However, the 2D bulk gaps in those quantum wells are extremely small, greatly limiting potential application in future electronics and spintronics. Despite this limitation, 2D TIs with a large bulk gap attracted plenty of interest. In this paper, recent progress in searching for TIs with a large bulk gap is reviewed briefly. We start by introducing some theoretical predictions of these new materials and then discuss some recent important achievements in crystal growth and characterization.

Keywords: two-dimensional topological insulators, large bulk energy gap, one-dimensional edge state

PACS: 73.20.–r, 71.15.–m, 73.61.Cw **DOI:** 10.1088/1674-1056/25/11/117312

1. Introduction

Since the invaluable concept of Fermi liquid was introduced and Bloch waves were proposed by Landau and Bloch, great progress has been made in understanding the electronic properties of crystals by band theory based on the single-particle scenario. According to the band theory, band insulators are crystals that cannot conduct current because the energy bands (valence band) below the Fermi level are fully occupied, while the bands (conduction band) above the Fermi level are completely empty. There is an energy gap between the valence band and the conduction band. When the gap is relatively small ($\sim$ 1 eV for silicon), we have well-known semiconductors that are the foundational materials of today's information technology. With the rapid development of the semiconductor industry, we will eventually confront some fundamental problems. One of those is the heat problem. With increasing density of integrated circuits, chips generate more and more heat, resulting in a huge waste of energy that will strongly affect chips' function sooner or later. Many physicists are trying to find new mechanisms that could resolve or mitigate the heat problem. In 2005 and 2006, the quantum spin Hall effect (2D TI) was proposed by Kane and Mele,[1] and Zhang *et al.*[2] Topological insulators are classified by the topological invariant Z_2. The key phenomenon in realizing TIs is band inversion. We will not discuss the theoretical description and definition of the topological invariant of TIs here, as details can be found in the previous review papers by Kane,[3] Zhang[4] and their coauthors. The first material that was proposed to be a 2D TI was grapheme.[1] Kane and Mele showed that in the edge of a piece of graphene there is a 1D topological edge state. The bulk energy gap in graphene is caused by spin–orbital coupling (SOC). It is well known that SOC is proportional to the atomic number (weight). Carbon atoms are very light, so the bulk gap in graphene is extremely tiny. In fact, the gap of graphene is much smaller than 1 meV. In practice, no one has been able to detect the predicted 1D topological edge state in graphene. Bernevig *et al.* proposed a previously unknown 2D TI system based on HgTe/CdTe quantum wells,[2] and their predictions were confirmed by low temperature transport measurements in 2007 by Molenkamp's group.[5] Later, Liu *et al.* predicted another quantum well (InAs/GaSb) to be a 2D TI.[6] In 2011, Du group succeeded in realizing InAs/GaSb bilayers and observed the 1D edge state.[7,8] The transport results of HgTe/CdTe and InAs/GaSb are shown in Fig. 1. Quantum resistance was clearly detected in both wells under very low temperature, which proved that electrons do move along a 2D TI's edge without energy dissipation. However, the bulk gap of HgTe/CdTe is about 10 meV and in InAs/GaSb it is even smaller, so dissipation-free transport can only occur in these materials at extremely low temperature, hindering their application. So improving the working temperature has become one of the key issues in the field of 2D TIs. In the last several years, great efforts have been made, seeking to move in this direction.

*Project supported by the National Natural Science Foundation of China (Grant Nos. U1632272, 11574201, and 11521404). D. Q. acknowledges support from the Changjiang Scholars Program, China and the Program for Professor of Special Appointment (Eastern Scholar), China.

†Corresponding author. E-mail: dqian@sjtu.edu.cn

© 2016 Chinese Physical Society and IOP Publishing Ltd

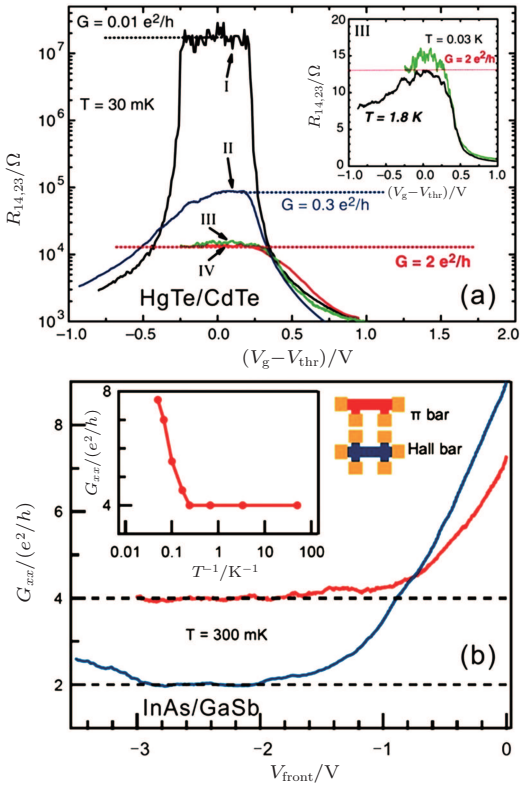


Fig. 1. (color online) (a) The longitudinal four-terminal resistance of HgTd/CdTe quantum wells as a function of gate voltage measured at $T = 30$ mK, from Ref. [5]. Device I is a topologically trivial quantum well. Devices II, III, and IV are topologically nontrivial quantum wells. In device IV (1.0 μm×0.5 μm), at suitable gate voltage, quantum resistance was observed. (b) Transport properties of the 1D edge states in InAs/GaSb bilayers, from Ref. [8]. Conductance plateaus quantized to $2e^2/h$ and $4e^2/h$, respectively, for the two device configurations shown in the inset, which both have length 2 μm and width 1 μm.

In this paper, we briefly review recent theoretical and experimental progresses in the study of 2D TIs with a large bulk energy gap. The paper is organized as follows. In Section 2, we introduce some theoretical predications of the new 2D materials that are 2D TIs with a very large gap. In Section 3, we discuss some recent experimental efforts in fabricating 2D TI materials and detecting the 1D edge states in 2D TI films as well as on the surface of particular bulk materials by angle-resolved photoemission spectroscopy (ARPES), scanning tunneling spectroscopy (STM), and transport measurements. In conclusion (Section 4), we discuss some issues and present our outlook.

2. New 2D TIs with a large energy gap predicted by first-principles calculations

2.1. Single-element 2D TIs with a large energy gap

Unlike quantum wells, 2D films consisting of a single element can be used to realize 2D TIs with a large energy gap. We introduce two samples below.

2.1.1. Bismuth (111) ultrathin films

Bismuth (Bi) is a heavy element with a very large SOC. Bulk Bi crystal has a rhombohedral structure and is well known for its novel spin-split surface states arising from the large SOC.[9] Along the (111) direction, the stable and smallest unit of Bi is the bilayer (BL) structure shown in Fig. 2(a). It is a buckled honeycomb-like structure. In theory, ultrathin Bi(111) BLs exhibit a semiconductor to semimetal transition with increasing thickness, and the crossover thickness is 4 or 5 BLs.[10,11] Band inversion happens at the Γ point (Brillouin zone center) in ultrathin Bi(111) films due to the large SOC. Parity analysis according to density functional theory (DFT) calculations shows that ultrathin Bi(111) (< 4 or 5 BLs) films are 2D TIs. The most interesting case is single-BL Bi(111), an indirect topologically nontrivial semiconductor. The energy gap of 1-BL Bi(111) is about 0.5 eV (Fig. 2(b)). The topological properties of 1-BL Bi(111) have been confirmed experimentally. We will discuss it in Section 3.

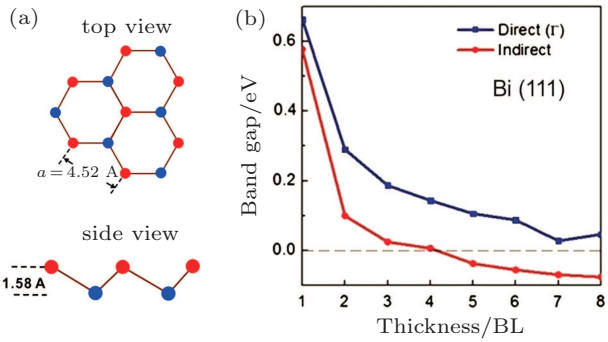


Fig. 2. (color online) (a) Top and side views of single-bilayer Bi(111). (b) Calculated energy gap of ultra-thin Bi(111) film as a function of thickness, from Ref. [11]. For single-bilayer Bi(111), the energy gap is larger than 0.5 eV.

2.1.2. Atomic octagonally tiled Bi ultra-thin films

Beyond buckled-honeycomb Bi, 2D Bi allotropes composed of eight-atom rings were recently reported by Li *et al.*[12] These allotropes contain unique atomic octagonal tiling (OT), as shown in Fig. 3(a). According to DFT calculations, OT-Bi is an indirect semiconductor with an energy gap of ~ 0.33 eV. The rather large gap is due to the strong SOC, and the interesting OT structure may provide Bi–Bi distances

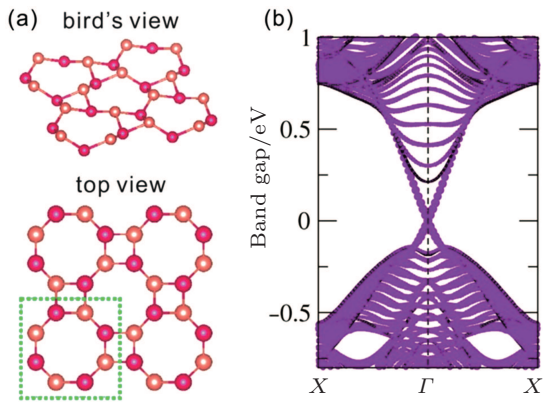


Fig. 3. (color online) Crystal and electronic structures of OT-Bi, from Ref. [12]. (a) Bird's-eye and side views of OT-Bi single-layer. (b) Bulk electronic bands and the Dirac-cone-like 1D edge state in the OT-Bi nanoribbon.

suited to the strong SOC. Calculations of the topological invariant and the edge state show that OT-Bi is a 2D TI material. Figure 3(b) presents the band structures of the OT-Bi ribbon, wherein gapless edge states clearly appear.

2.1.3. Single-BL Sn (111) films (stanene)

As we discussed in the introduction, graphene is the first 2D TI to be investigated, but its bulk energy gap is too small for electronic/spintronic application. Following the success with graphene, various 2D group IV materials with honeycomb lattices were fabricated, including a silicon counterpart of graphene (silicene),[13] a germanium graphene analogue (germanene),[14] and a tin graphene analogue (stanene).[15] Theoretically, silicene, germanene, and stanene are all 2D TIs.[16,17] The bulk energy gaps of silicene and germanene are relatively small, ~ 0.0016 eV and 0.024 eV, respectively. But the bulk energy gap of stanene is much larger, ~ 0.1 eV. The crystal structure of stanene is shown in Fig. 4(a). Similar to Bi(111), in top view, it has a honeycomb lattice. In side view, its atoms are not in a single plane. It has what is commonly called a buckled structure. The distance between two atomic layers (buckling distance) is about 1. The energy gap exists at K (K') points where band inversion happens. Graphene has sp^2 orbitals, but stanene has sp^3 orbitals that present dangling bonds on both sides of stanene. DFT calculations by Xu *et al.* show that the energy gap can be enhanced to about 0.3 eV by surface decoration.[17] After surface decoration, the dangling bonds are saturated, and the bulk energy gap moves to the Γ point. Band inversion happens at the Γ point after decoration by I, Br, F, OH, and others, but not in the case of hydrogen decoration.[17] Figure 4(c) shows the topological properties and bulk energy gap of stanene after surface decoration with different atoms.

2.2. Binary compound 2D TIs with large energy gaps

Besides single-element 2D semiconductors, binary 2D crystals can also be used to create 2D TIs. Just as we did for the single-element case, below, we introduce two typical examples of binary compounds that have been used.

2.2.1. Layered Bi_4Br_4

Bulk $Bi_4Br_4$is a layered material. It is a trivial insulator. Its interlayer bonding energy is comparable to those of other layered materials that have been successfully exfoliated, such as graphite and MoS_2. The topological properties of single-layer Bi_4Br_4 are completely different from those of its bulk parent material. Figure 5(a) shows the crystal structure of single-layer Bi_4Br_4, which has an infinite 1D molecular chain as its building block. Zhou *et al.* performed first-principles calculations for the material's band structure and topological invariant.[18] Single-layer Bi_4Br_4 is found to be a 2D TI. The bulk energy gap is about 0.18 eV. The band structure and the edge state of a single-layer Bi_4Br_4 nanoribbon are shown in Fig. 5(b). A single Dirac-cone edge state locates near the Γ point. As shown in Fig. 5(c), an external strain can effectively modify the band gap of single-layer Bi_4Br_4. The topological

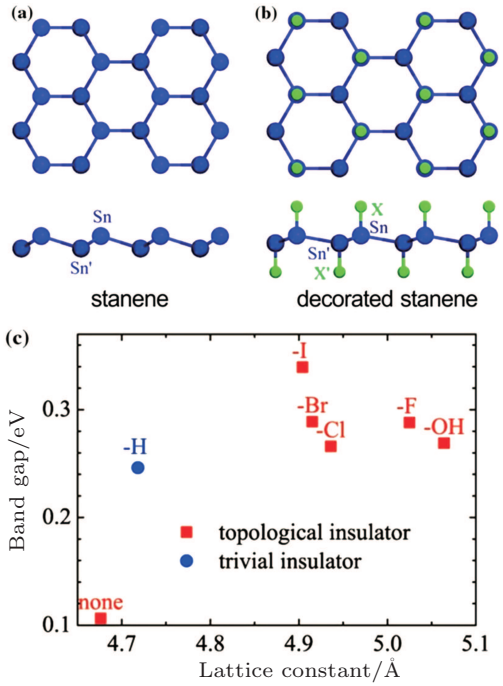


Fig. 4. (color online) Crystal structure and energy gap of stanene, from Ref. [17]. (a) Top and side views of stanene. (b) Top and side views of decorated stanene. (c) Energy gaps and topological properties of stanene and decorated stanene. Stanene has a bulk gap of ~ 0.1 eV. After decoration, the bulk gap increases to ~ 0.3 eV.

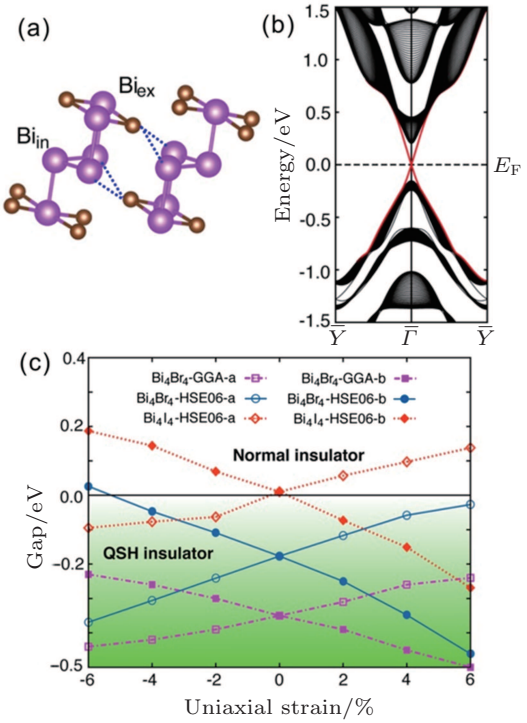


Fig. 5. (color online) Crystal and electronic structures of single-layer Bi_4Br_4, from Ref. [18]. (a) Unit cell of single-layer Bi_4Br_4. (b) Bulk electronic bands and the 1D edge state in Bi_4Br_4 nanoribbon. (c) Energy gap of single-layer Bi_4Br_4 as a function of external strain.

properties are robust. Interestingly, a similar compound Bi_4I_4 is near the phase transition boundary between topologically trivial and topologically nontrivial (Fig. 5(c)).

2.2.2. Layered compound $ZrTe_5$

Bulk $ZrTe_5$ is known as a layered thermoelectric material. The interlayer bonding in $ZrTe_5$ is only slightly stronger than that in graphite. Figure 6 shows the bulk crystal structure of $ZrTe_5$.[19] A layer is in the *a*–*c* plane. Weng *et al.* performed band calculations that suggest that bulk $ZrTe_5$ is very close to the boundary between weak and strong 3D TIs. But single-layer $ZrTe_5$ is a 2D TI with an energy gap of ~ 0.1 eV.[19] Figure 6(b) shows the bulk bands and the edge states from two different edges in $ZrTe_5$ nanoribbons. Two Dirac cones (red and blue) from different edge morphologies ($ZrTe_3$ prismatic chain and Te zigzag chain) appear clearly in the calculations.[19] Weng *et al.* also showed that the band inversion happens at the Γ point between the zigzag chain Te^z-p_x and the prism chain dimer Te^z-p_y states. Unlike other TIs such as Bi_2Se_3, the band inversion in single-layer $ZrTe_5$ is not due to SOC; it is due to special nonsymmorphic space group features.

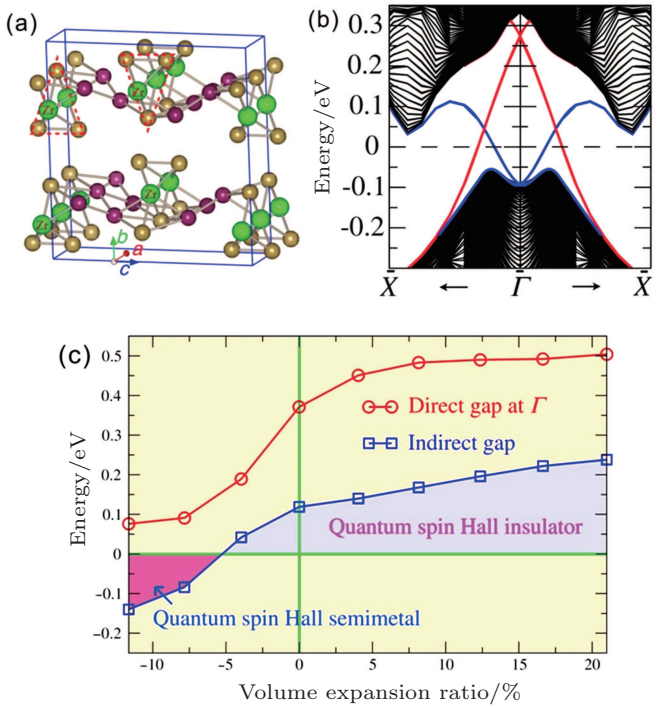


Fig. 6. (color online) Crystal and electronic structures of single-layer $ZrTe_5$, from Ref. [19]. (a) Bulk unit cell of $ZrTe_5$. $ZrTe_5$ layer is in the *a*–*c* plane. (b) Bulk electronic bands and the 1D edge states in single-layer $ZrTe_5$ nanoribbon. Red and blue curves are from two different edge morphologies. (c) Energy gap of single-layer $ZrTe_5$ as a function of external strain.

3. Experimental progress with large-gap 2D TIs

In Section 2, we briefly discussed some large-gap 2D TIs recently predicted by first-principles calculations. In the last several years, some of those have been successfully fabricated and their non-trivial topological properties were confirmed. Below, we discuss the recent progress.

3.1. Ultrathin Bi(111) films grown by molecular beam epitaxy (MBE)

Single-BL Bi(111) film is the first system that was carefully explored experimentally. Between 2011 and 2012, high quality ultrathin (< 5 BL) Bi(111) films were successfully grown for the first time, on Bi_2Te_3 substrates, using MBE, by two groups working independently.[20,21] Figure 7(a) shows the typical surface morphology of 1-BL Bi(111) films. The inset shows the hexagonal lattice of the surface layer. By combining ARPES and DFT calculations, Hirahara *et al.* suggested that despite some hybridization between Bi and the surface state of Bi_2Te_3, the topological properties of Bi(111) are retained.[20] Single-BL Bi(111) on Bi_2Te_3 substrate is topologically nontrivial. Yang *et al.* found a 1D edge state on 1-BL as well as on 2-BL films.[21] The bands measured by ARPES along one high-symmetry direction (*M*–Γ–*M*) and the corresponding DFT calculations are shown in Fig. 7(b). They agree very well. Both the real-space position and the energy position of the 1D edge state were successfully determined by STM/STS measurements. In Fig. 7(c), the energy position of the 1D state is presented. Due to charge transfer between Bi and the substrate, the energy gap is above the Fermi level (Fig. 7(c) upper and middle panels). The 1D edge state does exist in the 2D bulk energy gap (Fig. 7(c) bottom panel). Because of the state of the substrate, the Bi 2D gap cannot directly determined by STS. Since the agreement between calculations and ARPES spectra are so good, the 2D bulk gap of 1-BL Bi was extracted from DFT calculations. The energy gap is about 0.1 eV. This gap is smaller than that of free-standing

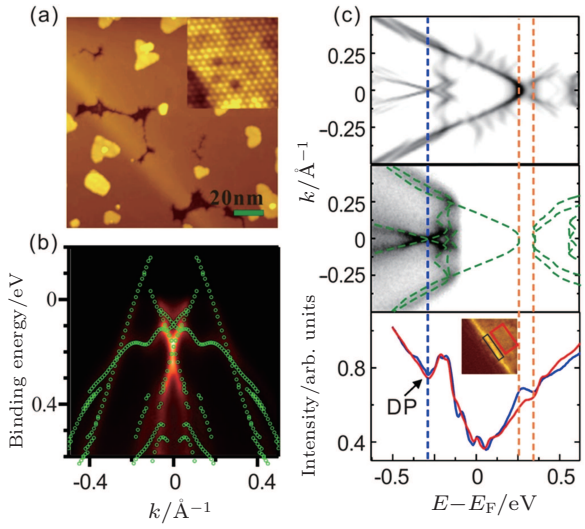


Fig. 7. (color online) Surface morphology and electronic structure of single-bilayer Bi(111) films grown on Bi_2Te_3, from Ref. [21]. (a) STM morphology of single-bilayer Bi(111)/Bi_2Te_3. (b) ARPES spectra overlaid with DFT calculations. (c) 1D edge state and bulk energy gap of single-bilayer Bi(111)/Bi_2Te_3.

1-BL Bi because the in-plane lattice constant of the real film is smaller ($\sim 4\%$) than that of free-standing films. If we can grow Bi on some other substrate that has a large lattice constant, the energy gap can be greatly increased.

3.2. 1-BL Bi(111) on the surface of bulk Bi

Besides the epitaxial films, the topological properties of the nearly free-standing Bi(111) have also been explored on the surface of bulk Bi. Drozdov *et al.* studied the edge states of 1-BL islands on the surface of bulk Bi.[22] Figure 8 presents the main findings from Ref. [22]. As shown in Fig. 8(a), along its [111] direction, bulk Bi can be considered as a stack of Bi BLs that are weakly bonded to each other. In 1-BL Bi islands on the surface, there can be Klein, armchair, or zigzag edges. Only zigzag edges are suitable for detection of a 1D edge state. A zigzag edge has either of two forms, type-A and type-B, as shown in Fig. 8(a). In a type-A edge, the terminating Bi is close to vacuum, while in a type-B edge, it is close to the bulk layer. DFT calculations show that the 1D topological edge state in the type-A edge is weakly hybridized with the bulk states and therefore detectable by STM/STS. Figure 8(b) shows the STS spectra at three different positions: terrace, type-A edge, and type-B edge. Obviously, there are no sharp features on the type-B edge. But very sharp features are observed on the terrace ($E_1 = 213$ meV) and on the type-A edge ($E_2 = 183$ meV). By fitting the line shape of these two peaks, the peak at E_1 is attributed to a 2D surface state of bulk Bi and the peak at E_2 represents a 1D edge state. Quasi-particle interference measurements were carried out to determine the origins of E_1 and E_2. Two dispersive features (q_1 and q_2) were obtained, as shown in Fig. 8(c). Those features agree well with the first-principles calculations. Peak E_1 (or q_1) corresponds to the band maximum of the 1D edge state, while peak E_2 (or q_2) is related to the saddle point of the 2D surface band.

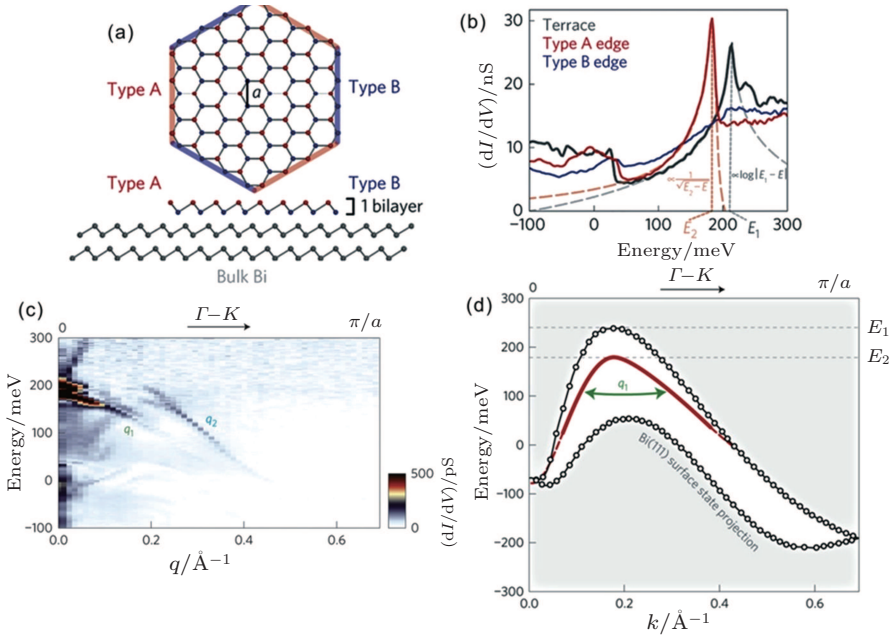


Fig. 8. (color online) 1D edge state in single-bilayer Bi islands on the surface of bulk Bi, from Ref. [22]. (a) Schematics of Bi-bilayer's atomic structure. Two types of edges are marked by red and blue lines, respectively. (b) STS of type-A and type-B edges, as well as of the terrace. (c) Quasi-particle interference within the edge channel. Two branches were observed: q_1 and q_2 come from the 1D edge state and 2D surface state, respectively. (d) Schematic of the band dispersion for the Bi bilayer on bulk Bi(111). The grey region represents the projected Bi(111) surface state continuum in the direction parallel to the 1D edge state. E_1 and E_2 indicate the peak positions in panel (b).

3.3. Nanoscale transport measurements of free-standing 1-BL Bi(111)

Although spectral measurements of both thin films and bulk crystals confirmed the non-trivial TI property of 1-BL Bi(111), transport measurement cannot been done on the films or on the surface of bulk Bi because they are not in the insulating state. In 2013, Sabater *et al.* tried to measure the transport properties of a free-standing 1-BL Bi layer on a Bi nanocontact.[23] Figure 9 shows their main conclusions. Figure 9(a) shows the proposed process of exfoliating a Bi(111) bilayer after contact with the STM tip. The gray parts are the tip and the bulk Bi. The red part is 1-BL Bi exfoliated from the bulk. These experiments were carried out at room temperature in air. Two-terminal conductance of the nanoscale 1-BL Bi layer was measured between the STM tip and the bulk Bi as a function of the tip retraction distance. Surprisingly, as shown in Fig. 9(b), large conductance plateaus at quantum conductance G_0 were observed in some samples. The frequency of finding these plateaus may reflect the topological properties of the 1D edge state, although other interpretations cannot be completely ruled out. The exact mechanism is still controversial, but the experimental results do show extraordinary behaviors: (i) the quantum conductance cannot be associated with single-atom contact, but must be associated with a nanoscopic

constriction, (ii) it appears at room temperature and is robust despite the presence of a small concentration of contaminants in the air.

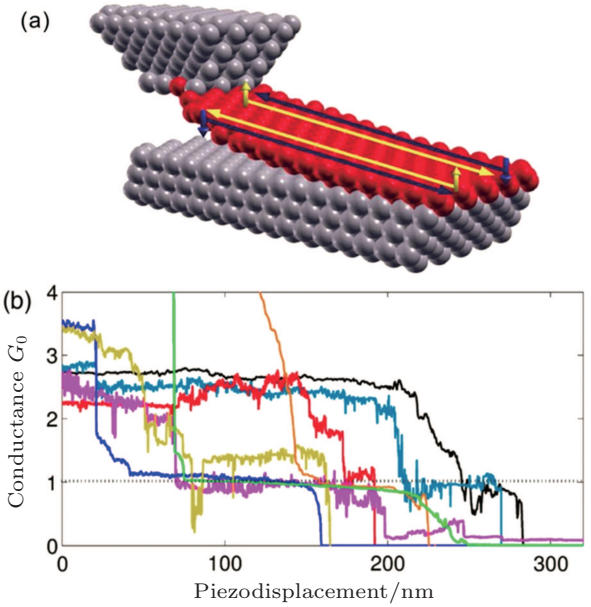


Fig. 9. (color online) Conductance of Bi nanocontact, from Ref. [23]. (a) The proposed process of exfoliating a Bi(111) bilayer (red) after contact with the STM tip. (b) Conductance plateaus of Bi(111) bilayers between tip and substrate.

3.4. Realization of 2D stanene films by MBE

Stanene has a crystal structure similar to 1-BL Bi(111) films. However, the interaction between two stanene layers is very strong. In fact, a stack of stanene forms bulk grey tin with a diamond structure; hence it is impossible to isolate stanene by mechanical exfoliation. Bulk grey tin is not stable at room temperature. In 2015, Zhu *et al.* succeeded in growing 2D stanene films by MBE. The crystal structure of stanene and its electronic structures were determined for the first time. Figure 10 shows the main results of that work.[15] Ulrathin tin films were grown on the Bi_2Te_3 substrate. The hexagon lattice was observed by STM (Fig. 10(a)). Where the coverage was low, near the edge of some islands, two atomic tin layers were also resolved. A model of the crystal structure of the epitaxial stanene, in accord with the experimental data, is shown in Fig. 10(b). The orange and green balls represent the top and bottom atomic tin layers, respectively. The big grey balls are the Te atoms of the substrate's surface. The electronic bands of stanene are presented in Fig. 10(c), wherein the blue dots come from stanene and the other features come from the substrate. In the experiment, the dangling bonds of stanene were found to be saturated during the growth process. Bands calculated based on the lattice parameter determined by the experiments agree well with the ARPES spectra. DFT calculations show that the band hybridization between stanene and the substrate is weak, except for some charge transfer.[15] No topological property of stanene has been confirmed so far.

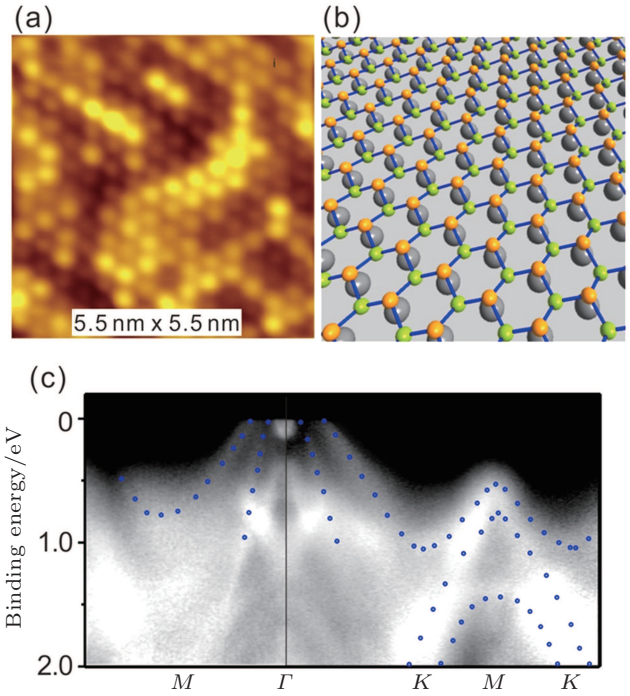


Fig. 10. (color online) Crystal and electronic structures of stanene, from Ref. [15]. (a) Hexagonal lattice of the stanene surface. (b) Lattice model of stanene on Bi_2Te_3 substrate. Orange and green balls represent stanene atoms. Grey balls represent Te atoms. (c) ARPES spectra of stanene/Bi_2Te_3. Blue dotted lines mark stanene bands.

3.5. Single-layer $ZrTe_5$ on the surface of bulk $ZrTe_5$

Although no single-layer $ZrTe_5$ film or free-standing layer has been obtained yet, the topological properties of single-layer $ZrTe_5$ were confirmed by observation of a 1D

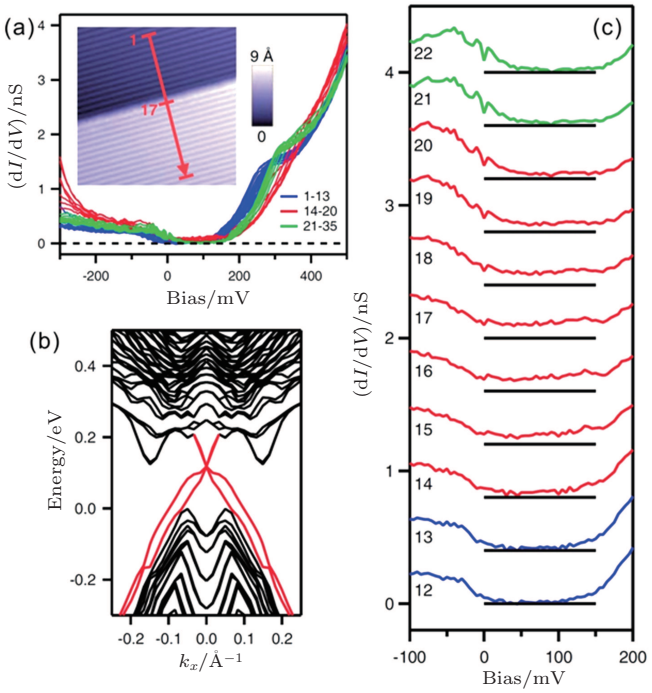


Fig. 11. (color online) 1D edge state in the step edge of a single-layer $ZrTe_5$ island on the surface of bulk $ZrTe_5$, from Ref. [24]. (a) Morphology of single-layer $ZrTe_5$ step. STS curves obtained from the terrace and the edge. (b) Calculated bulk bands and 1D edge state of a single-layer $ZrTe_5$ nanoribbon. (c) Full energy gap observed on the terrace. Contributions from 1D edge state were observed near the edge (red curves).

edge on the surface of bulk $ZrTe_5$ with the help of DFT calculations. Two groups independently carried out the experiments.[24,25] Figure 11 shows the main findings from Ref. [24]. On the cleaved surface of bulk $ZrTe_5$, a sharp edge was observed, as shown in Fig. 11(a). Similar to studies of bulk Bi, STS were taken on the terrace as well as on the edge. In Fig. 11(c), lines 14 to 20 are STS near the edge. On the terrace, STS shows an energy gap of about 0.1 eV that is consistent with DFT calculations (Fig. 11(b)). Within the bulk gap, conductance is zero on the terrace, within the bounds of experimental uncertainty. But around the edge, conductance is not zero within the bulk gap. Some weak features appear in Fig. 11(c) (red curves). Many sharp features were identified by another group.[25] Unlike bulk Bi, the 1D edge state of $ZrTe_5$ can be detected on all edges, independent of the edge geometry.[25] STS measurements confirm that single-layer $ZrTe_5$ is a 2D TI with a large energy gap (~ 0.1 eV). Since $ZrTe_5$ shows a full bulk gap, it is possible to undertake future studies of the edge transport on the surface of $ZrTe_5$.

3.6. One-dimensional edge state in $Bi_{14}Rh_3I_9$

Two-dimensional TIs can also be realized in a very complicated material that is a weak 3D TI in the bulk. Figure 12 presents a recent experiment on $Bi_{14}Rh_3I_9$ crystals by Pauly *et al.* using STS measurements.[26] The compound $Bi_{14}Rh_3I_9$ consists of two types of layers stacked alternately. One type of layer, $[(Bi_4Rh)_3I]^{2+}$, exhibits a honeycomb lattice formed by rhodium-centered Bi cubes;[27] the other type $[Bi_2I_8]^{2-}$, acts as a space layer, as shown in Fig. 12(a). According to DFT calculations, bulk $Bi_{14}Rh_3I_9$ is a weak 3D TI with a bulk gap of about 0.21 eV. On a cleaved surface, there are step edges (Fig. 12(b)). Near those edges, the 2D $(Bi_4Rh)_3I$ layer and the spacer Bi_2I_8 layer are both observable. STS on a terrace of the space layer shows an energy gap (blue curve in Fig. 12(c)). Similar to Bi and $ZrTe_5$, a sharp 1D state was observed on the edge of the $(Bi_4Rh)_3I$ layer. The energy gap on the 2D $(Bi_4Rh)_3I$, determined by STS, is about 0.18 eV, which is consistent with ARPES measurements.[27] The experiments on $Bi_{14}Rh_3I_9$, as well as on $ZeTe_5$, prove that a 1D topological edge state can exist on every step edge in 3D weak TI materials.

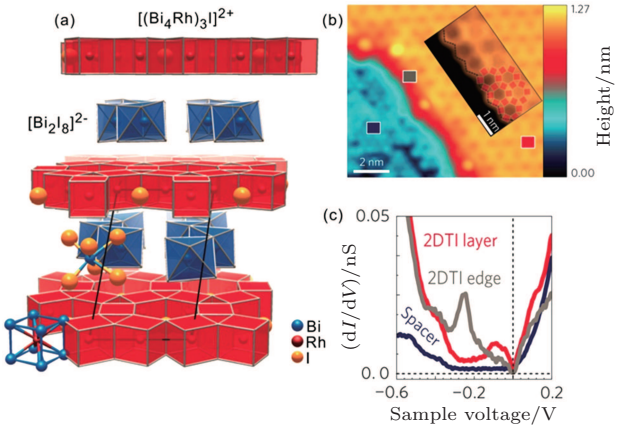


Fig. 12. (color online) Crystal structure and 1D edge state of 2D layer of $Bi_{14}Rh_3I_9$, from Ref. [26]. (a) $Bi_{14}Rh_3I_9$ consists of 2D $(Bi_4Rh)_3I$ layers alternating with Bi_2I_8 space layers. (b) On the cleaved surface, 2D layers and space layers are both observed. (c) STS of different positions. Sharp feature from 1D edge state was observed on the edge of 2D $(Bi_4Rh)_3I$ layer.

4. Discussion and outlook

We have briefly reviewed recent progress with the large gap 2D TIs, including single-BL Bi(111) films, stanene films, single-layer Bi_4Br_4, single-layer $ZrTe_5$, and single-layer $(Bi_4Rh)_3I$. Those systems all include heavy elements. Energy gaps in all these materials except $ZrTe_5$ are caused by the SOC, that is, a large SOC, which is inherent in the heavy elements, results in the large bulk gap. However, an energy gap induced by SOC cannot be very large. It would be extremely difficult to realize 2D TIs with a 1 eV gap purely due to SOC, even in theory. On the other hand, the gap in $ZrTe_5$ is due to its very special space group, which implies that it could be possible to obtain a larger bulk gap in nonsymmorphic crystals, regardless of the SOC.

Although nontrivial TI properties and 1D edge states have been confirmed in Bi, $ZrTe_5$, and $(Bi_4Rh)_3I$, it is still a big challenge to explore the electric transport properties along the 1D edge states at high temperature. In my view, Bi(111) film is currently the best possible candidate for transport measurements because Bi films are much more stable than stanene or $ZrTe_5$. So far, single-BL Bi can be realized only on the surface of Bi_2Te_3 (or similar compounds). The surface of Bi_2Te_3 consists of Te atoms with a hexagonal lattice. The lattice mismatch between the Te layer and Bi is moderate, which helps us obtain smooth single-BL Bi. On the other hand, Te layers are also inert, so there are no chemical bonds between Te and Bi. The topological properties of Bi are preserved despite some hybridization between the surface state of Bi_2Te_3 and the Bi. However, transport measurement of Bi/Bi_2Te_3 films is impossible because the substrate has metallic surface states. Several methods could be explored to overcome this problem. For example, we can use a single-layer Bi_2Te_3 film as the substrate. Due to quantum confinement, single-layer Bi_2Te_3 is a trivial insulator (gap ~ 0.2 eV). In addition, other semiconductors such as In_2Te_3 abd In_2Se_3 (gap ~ 1 eV) that have an inert surface layer similar to that of Bi_2Te_3 could be very good choices if we can obtain high quality films. In the next several years, one of the most important issues in the field of 2D TI is finding stable systems that can be fabricated to explore the electric transport properties along the 1D edge states at high temperature.

References

[1] Kane C L and Mele E J 2005 *Phys. Rev. Lett.* **95** 226801

[2] Bernevig B A, Hughes T L and Zhang S C 2006 *Science* **314** 1757
[3] Hasan M Z and Kane C L 2010 *Rev. Mod. Phys.* **82** 3045
[4] Qi X L and Zhang S C 2011 *Rev. Mod. Phys.* **83** 1057
[5] Koenig M, Wiedmann S, Bruene C, Roth A, Buhmann H, Molenkamp L W, Qi X L and Zhang S C 2007 *Science* **318** 766
[6] Liu C, Hughes T, Qi X L, Wang L and Zhang S C 2008 *Phys. Rev. Lett.* **100** 236601
[7] Knez I, Du R R and Sullivan G 2011 *Phys. Rev. Lett.* **107** 136603
[8] Du L, Knez I, Sullivan G and Du R R 2015 *Phys. Rev. Lett.* **114** 096802
[9] Hofmann P 2006 *Prog. Surf. Sci.* **81** 191
[10] Koroteev Y M, Bihlmayer G, Chulkov E V and Blugel S 2008 *Phys. Rev. B* **77** 045428
[11] Liu Z, Liu C X, Wu Y S, Duan W H, Liu F and Wu J 2011 *Phys. Rev. Lett.* **107** 136805
[12] Li P and Luo W D 2016 *Sci. Rep.* **6** 25423
[13] Vogt P, Padova P D, Quaresima C, Avila J, Frantzeskakis E, Asensio M C, Resta A, Ealet B and Lay G L 2012 *Phys. Rev. Lett.* **108** 155501
[14] D'avilla M E, Xian L, Cahangirov S, Rubio A and Lay G L 2014 *New J. Phys.* **16** 095002
[15] Zhu F F, Chen W J, Xu Y, Gao C L, Guan D D, Liu C H, Qian D, Zhang S C and Jia J F 2015 *Nat. Mater.* **14** 1020
[16] Liu C C, Jiang H and Yao Y G 2011 *Phys. Rev. B* **84** 195430
[17] Xu Y, Yan B, Zhang H J, Wang J, Xu G, Tang P, Duan W H and Zhang S C 2013 *Phys. Rev. Lett.* **111** 136804
[18] Zhou J J, Feng W, Liu C C, Guan S and Yao Y G 2014 *Nano Lett.* **14** 4767
[19] Weng H, Dai X and Fang Z 2014 *Phys. Rev. X* **4** 011002
[20] Hirahara T, Bihlmayer G, Sakamoto Y, Yamada M, Miyazaki H, Kimura S, Blugel S and Hasegawa S 2011 *Phys. Rev. Lett.* **107** 166801
[21] Yang F, Miao L, Wang Z F, Yao M Y, Zhu F F, Song Y R, Wang M X, Xu J P, Fedorov A V, Sun Z, Zhang G B, Liu C H, Liu F, Qian D, Gao C L and Jia J F 2012 *Phys. Rev. Lett.* **109** 016801
[22] Drozdov I K, Alexandradinata A, Jeon S, Nadj-Perge S, Ji H, Cava R J, Bernevig B A and Yazdani A 2014 *Nat. Phys.* **10** 664
[23] Sabater C, Gosalbez-Martınez D, Fernandez-Rossier J, Rodrigo J G, Untiedt C and Palacios J J 2013 *Phys. Rev. Lett.* **110** 176802
[24] Wu R, Ma J Z, Nie S M, Zhao L X, Huang X, Yin J X, Fu B B, Richard O, Chen G F, Fang Z, Dai X, Weng H M, Qian T, Ding H and Pan S H 2016 *Phys. Rev. X* **6** 021017
[25] Li X, Huang W, Lv Y, Zhang K, Yang C, Zhang B, Chen Y B, Yao S, Zhou J, Lu M, Sheng L, Li S C, Jia J F, Xue Q K, Chen Y and Xing D Y 2016 *Phys. Rev. Lett.* **116** 176803
[26] Pauly C, Rasche B, Koepernik K, Liebmann M, Pratzer M, Richter M, Kellner J, Eschbach M, Kaufmann B, Plucinski L, Schneider C M, Ruck M, Brink J van den and Morgenstern M 2015 *Nat. Phys.* **11** 338
[27] Rasche B, Isaeva A, Ruck M, Borisenko S, Zabolotnyy V, Büchner B, Koepernik K, Ortix C, Richter M and Brink J. van den 2013 *Nat. Mater.* **12** 422